JOURNAL OF VIROLOGY, Jan. 2001, p. 878–890 Vol. 75, No. 2
0022-538X/01/$04.00+0 DOI: 10.1128/JVI.75.2.878–890.2001

Inducible Expression of Inflammatory Chemokines in Respiratory Syncytial Virus-Infected Mice: Role of MIP-1α in Lung Pathology

HELENE A. HAEBERLE,[1,2] WILLIAM A. KUZIEL,[3] HANS-JUERGEN DIETERICH,[2] ANTONELLA CASOLA,[1] ZORAN GATALICA,[4] AND ROBERTO P. GAROFALO[1,5]*

Departments of Pediatrics,[1] Pathology,[4] and Microbiology and Immunology,[5] The University of Texas Medical Branch, Galveston, and Department of Genetics and Microbiology, University of Texas, Austin,[3] Texas, and Department of Anesthesiology, Universitaetsklinikum, Tuebingen, Germany[2]

Received 15 May 2000/Accepted 13 October 2000

Lower respiratory tract disease caused by respiratory syncytial virus (RSV) is characterized by profound airway mucosa inflammation, both in infants with naturally acquired infection and in experimentally inoculated animal models. Chemokines are central regulatory molecules in inflammatory, immune, and infectious processes of the lung. In this study, we demonstrate that intranasal infection of BALB/c mice with RSV A results in inducible expression of lung chemokines belonging to the CXC (MIP-2 and IP-10), CC (RANTES, eotaxin, MIP-1β, MIP-1α, MCP-1, TCA-3) and C (lymphotactin) families. Chemokine mRNA expression occurred as early as 24 h following inoculation and persisted for at least 5 days in mice inoculated with the highest dose of virus (10^7 PFU). In general, levels of chemokine mRNA and protein were dependent on the dose of RSV inoculum and paralleled the intensity of lung cellular inflammation. Immunohisthochemical studies indicated that RSV-induced expression of MIP-1α, one of the most abundantly expressed chemokines, was primarily localized in epithelial cells of the alveoli and bronchioles, as well as in adjoining capillary endothelium. Genetically altered mice with a selective deletion of the MIP-1α gene (−/− mice) demonstrated a significant reduction in lung inflammation following RSV infection, compared to control littermates (+/+ mice). Despite the paucity of infiltrating cells, the peak RSV titer in the lung of −/− mice was not significantly different from that observed in +/+ mice. These results provide the first direct evidence that RSV infection may induce lung inflammation via the early production of inflammatory chemokines.

Respiratory syncytial virus (RSV) is the major cause of serious lower respiratory disease in infancy and early childhood (5). Bronchiolitis, the more severe clinical manifestation of RSV infection, is characterized by necrosis and sloughing of the respiratory epithelium and plugging of the small bronchioles with fibrin and mucus. An intense peribronchial infiltration of mononuclear cells (lymphocytes and monocytes) occurs, with considerable edema (1, 8, 10). In addition, presence of the granule-associate cytotoxic proteins histamine, eosinophil cationic protein, and major basic protein in nasopharyngeal secretions and tracheobronchial aspirates suggests that RSV infection triggers the migration to the airways and activation of basophils and eosinophils (12, 17, 37, 46). The evidence of an inverse correlation between the levels of these cytotoxic mediators and the degree of oxygen saturation in RSV-infected infants further underscores the critical role played by mucosal inflammation in the pathogenesis of RSV airway disease (12, 45, 46).

The mouse model shows close similarity to the pathogenesis of RSV-induced lower airway disease in humans. In BALB/c mice, RSV rapidly replicates in the lungs after intranasal inoculation, and induces mononuclear cell infiltration around peribronchial and perivascular tissues (41) and objective plethysmographic signs of pulmonary dysfunction (i.e., increased respiratory rates and airway hyperresponsiveness) (29, 44). These pathophysiologic changes correlate with the amount of viral inoculum (44), consistent with the observation that more severe disease occurs in infected children who have higher concentrations of RSV in their secretions (4, 16).

The mechanisms that regulate selective recruitment of inflammatory cells to the airways and their activation following RSV infection are still largely unknown. Similarly, virus- or host-specific factors that may influence these events have not been yet identified. Much of the cellular response at sites of tissue inflammation is controlled by gradients of chemotactic factors that direct leukocyte transendothelial migration and movement through the extracellular matrix. The composition of this cellular response is dependent upon the discrete target cell selectivity of these chemotactic molecules. Chemokines, a superfamily of small chemotactic cytokines, have emerged as central regulatory molecules in inflammatory, immune, and infectious processes of the lung (28). Chemokines have been primarily divided into two main subfamilies, CXC (α) and CC (β), upon their sequence homology and the position of the first two cysteine residues. In general, this subdivision is mirrored by the activity of these two chemokine groups on neutrophils (CXC) or monocytes, eosinophils, and basophils (CC). However, within the CXC subfamily, chemokines such as gamma interferon-inducible protein-10 (IP-10) that lack the amino acid motif ELR (glutamic acid-leucine-arginine) in the NH_2 terminal domain, do not bind the CXCR1 and CXCR2 receptors (the interleukin-8 [IL-8] receptors) on neutrophils. Instead, the IP-10 receptor, CXCR3, is expressed on most peripheral blood memory T cells and NK cells (30). In addition, another subgroup of chemokines, the C family, which contain

* Corresponding author. Mailing address: Division of Immunology/Allergy/Rheumatology, 301 University Blvd., Galveston, TX 77555-0369. Phone: (409) 772-2658. Fax: (409) 772-1761. E-mail: rpgarofa@utmb.edu.

one instead of two cysteines in the N terminus domain, has been recently described. Lymphotactin (Ltn), a still poorly characterized selective attractant for lymphocytes, is one of the two members of this group (19).

A number of studies have shown that RSV is among the most potent stimuli to induce production of CXC and CC chemokines by epithelial cells (3, 13, 26, 32). Chemokine release in nasopharyngeal secretions has also been reported in infants with RSV infection (17, 36). However, given the ethical and procedural difficulties in performing invasive studies in young infants infected by RSV, no information is available on the spectrum, kinetics, and viral-dose dependence of chemokine expression in the lower airways, as well as the histopathologic features associated with their production. To address these questions, we have characterized the expression of inducible chemokines in the lung of RSV-infected BALB/c mice. Moreover, using mice bearing a selected disruption of the gene encoding for the CC chemokine MIP-1α, we have investigated the role of MIP-1α in mediating airway inflammation following RSV infection.

MATERIALS AND METHODS

RSV preparation. The human long strain of RSV (A2) was grown in HEp-2 cells (American Type Culture Collection [ATCC], Manassas, Va.). RSV was purified by polyethylene glycol precipitation, followed by centrifugation on 35 to 65% discontinuous sucrose gradients as described elsewhere (26, 43). The virus was aliquoted, quick frozen, and stored at −70°C until used. The virus titer was determined by a methylcellulose plaque assay (20). No contaminating cytokines, including IL-1, IL-6, IL-8, tumor necrosis factor alpha, granulocyte-macrophage colony-stimulating factor (GM-CSF), and interferons were found in the sucrose-purified viral preparations (18).

Mice and infection protocol. Female, 4- to 6-week-old BALB/c mice were purchased from Harlan (Houston, Tex.) and were housed under pathogen-free conditions in the animal research facility of the University of Texas Medical Branch (UTMB), Galveston, Tex., in accordance with the National Institutes of Health and UTMB institutional guidelines for animal care. C57BL/6J × 129 Ola MIP-1α$^{-/-}$ mice (6) were bred at the University of Texas, Austin. Cages, bedding, food, and water were sterilized before use. Under light anesthesia, mice were inoculated intranasally (i.n.) with 50 μl of purified RSV diluted in phosphate-buffered saline (PBS) (final administered doses: 5×10^5, 10^6, and 10^7 PFU). The 50 μl volume was selected to allow infection of the mice with a high titer of purified RSV and distribution of the inoculum mainly in the lung tissue (14). In separate experiments mice were inoculated with 10^7 PFU of UV-inactivated pRSV. Control mice were inoculated with the same volume of either PBS or supernatant from uninfected HEp-2 cells processed in the same way as infected cells used for the preparation of purified RSV (referred to herein as sham infection). In some experiments, total protein concentration was adjusted in the uninfected HEp-2 cell and RSV preparations to obtain an equal amount in the intranasal inoculum. The use of these control preparations gave similar results and therefore subsequent studies were performed with PBS-inoculated controls only. At the indicated time points after infection, mice were anesthetized with an intraperitoneal injection of ketamine and xylazine before the thoracic cavity was opened. To collect a bronchoalveolar lavage (BAL) sample, the mice were exsanguinated via heart puncture and the trachea was opened by incision of the cricothyroid membrane to flush the lungs twice with ice-cold sterile PBS (1 ml). Lungs were then removed for RSV titration, RNA isolation, and determination of chemokine proteins. For virus titration, the lungs were homogenized in Dulbecco's modified Eagle medium supplemented with 2% fetal calf serum in a 10% ratio (wt/vol). Homogenized samples were centrifuged at $2,000 \times g$ for 10 min. Serial dilutions of the supernatants were tested in a methylcellulose plaque assay (20).

Chemokine mRNA expression by RNAse protection assay. After excision, lungs were quick frozen in liquid nitrogen and stored at −80°C until total RNA was isolated by the thiocyanate-phenol chloroform method. Chemokine mRNA expression was determined by a multiprobe RNase protection assay (RPA) using the RiboQuant kit (Pharmingen, San Diego, Calif.). The multiprobe template mCK-5 contains DNA templates for the chemokines Ltn, RANTES, eotaxin, MIP-1β, MIP-1α, MIP-2, IP-10, MCP-1, TCA-3, and the housekeeping genes encoding L32 (ribosomal RNA) and GAPDH (glyceraldehyde-3-phosphate dehydrogenase). The probe was labeled with [α-^{32}P]UTP (3,000 Ci/mmol; 10 μCi/μl; Du Pont NEN Research Products, Boston, Mass.) using a T7 polymerase. After overnight hybridization with 10 μg of total RNA and RNA digestion, the samples were treated with proteinase K-sodium dodecyl sulfate mixture, extracted by phenol-chloroform, and precipitated in the presence of ammonium acetate. The samples were finally loaded on a QuickPoint sequence gel (Novex, San Diego, Calif.), exposed to an XAR film (Eastman Kodak), and developed at −70°C. The identity of each protected fragment was established by analyzing its migration distance against a standard curve of the migration distance versus the log nucleotide length for each undigested probe. The quantity of each mRNA species in the original RNA sample was then determined based on the signal intensity (measured by an AlphaImager 2200 optical densitometer [Alpha Innotech Corp., San Leandro, Calif.]) given by the appropriately sized, protected probe fragment bands. Sample loading was normalized to the housekeeping gene coding for GAPDH, included in each template set.

Determination of chemokine proteins in lung tissue extracts and BAL samples. Lungs were homogenized in lysis buffer (0.5% Triton X-100, 150 mM NaCl, 15 mM Tris, 1 mM $CaCl_2$, 1 mM $MgCl_2$). Homogenized tissue was kept on ice for 30 min before centrifugation ($850 \times g$ for 30 min). After filtration through a 0.2-μm-pore-size filter, supernatants were tested by commercial enzyme-linked immunosorbent assay (ELISA) kits for RANTES, MIP-1α (R&D Systems, Minneapolis, Minn.), and MCP-1 (Biosource International, Camarillo, Calif.). The sensitivities of the assay for RANTES, MIP-1α, and MCP-1 were 2, 1.5, and 9 pg/ml, respectively. BAL samples were centrifuged at $1,000 \times g$ for 10 min before determination of chemokines was performed.

Detection of MIP-1α in BALB/c lung tissue by immunohistochemistry. The thoracic cavity was opened and the lungs were flushed through an incision of the trachea with 1 ml of 50% optimum cutting temperature (OCT) compound in PBS. After ligation of the trachea, lungs were removed, embedded in 100% OCT compound, and snap-frozen in dry ice with 2-methylbutane (Sigma). Sections were cut onto slides, air dried, fixed in acetone, and stored at −70°C until staining for MIP-1α was performed. For the staining, the slides were washed in PBS and blocked for 1 h with gelatin (Sigma) at room temperature. After multiple washes in PBS the tissue was incubated overnight at 4°C with a purified goat anti-murine MIP-1α antibody (2 μg/ml; R&D Systems) diluted in gelatin. After multiple washings in PBS, bound antibody was detected with Alexa Fluor 488-labeled donkey anti-goat immunoglobulin G (IgG) antibody (Molecular Probes, Eugene, Oreg.). After a 1-h incubation at room temperature, the slides were washed in PBS and mounted with the ProLong Antifade Kit (Molecular Probes). The stained slides were analyzed by immunofluorescence microscopy. For negative controls, the same sections were treated accordingly but without the first antibody.

Pulmonary histopathology. Lungs were perfused and fixed in 10% buffered formalin and embedded in paraffin. Multiple 4-μm-thick sections were stained with haematoxylin & eosin (H&E). Slides were analyzed and scored for cellular inflammation under light microscopy by two independent pathologists, as previously described (24, 38). Briefly, inflammatory infiltrates were scored by enumerating the layers of inflammatory cells surrounding the vessels and bronchioles. Finding zero to three layers of inflammatory cells was considered normal. Finding moderate to abundant infiltrate (more than three layers of inflammatory cells surrounding 50% or more of the circumference of the vessel or bronchioles) was considered abnormal. The number of abnormal perivascular and peribronchial spaces divided by the total perivascular and peribronchial spaces was the percentage reported as the pathology score. A total of ~15 perivascular and peribronchial spaces per lung were counted for each animal.

Statistical analysis. Statistical analysis was carried out using the SigmaStat 3.0 program (Jandel Corp., San Rafael, Calif.). The data were analyzed by Wilcoxon test. Correlation was determined using the Spearman correlation test. If the data were not normally distributed statistical analysis was completed after logarithmic transformation of data.

RESULTS

Induction of chemokine mRNA in the lung of RSV-infected mice. To characterize the profile and abundance of lung chemokines that are expressed in vivo following RSV infection, groups of BALB/c mice were inoculated i.n. with three increasing doses of sucrose-purified RSV A (5×10^5, 10^6, and 10^7 PFU) or were sham-infected with PBS. Mice were sacrificed at days 1, 5, and 21 postinoculation; RNA was isolated from the

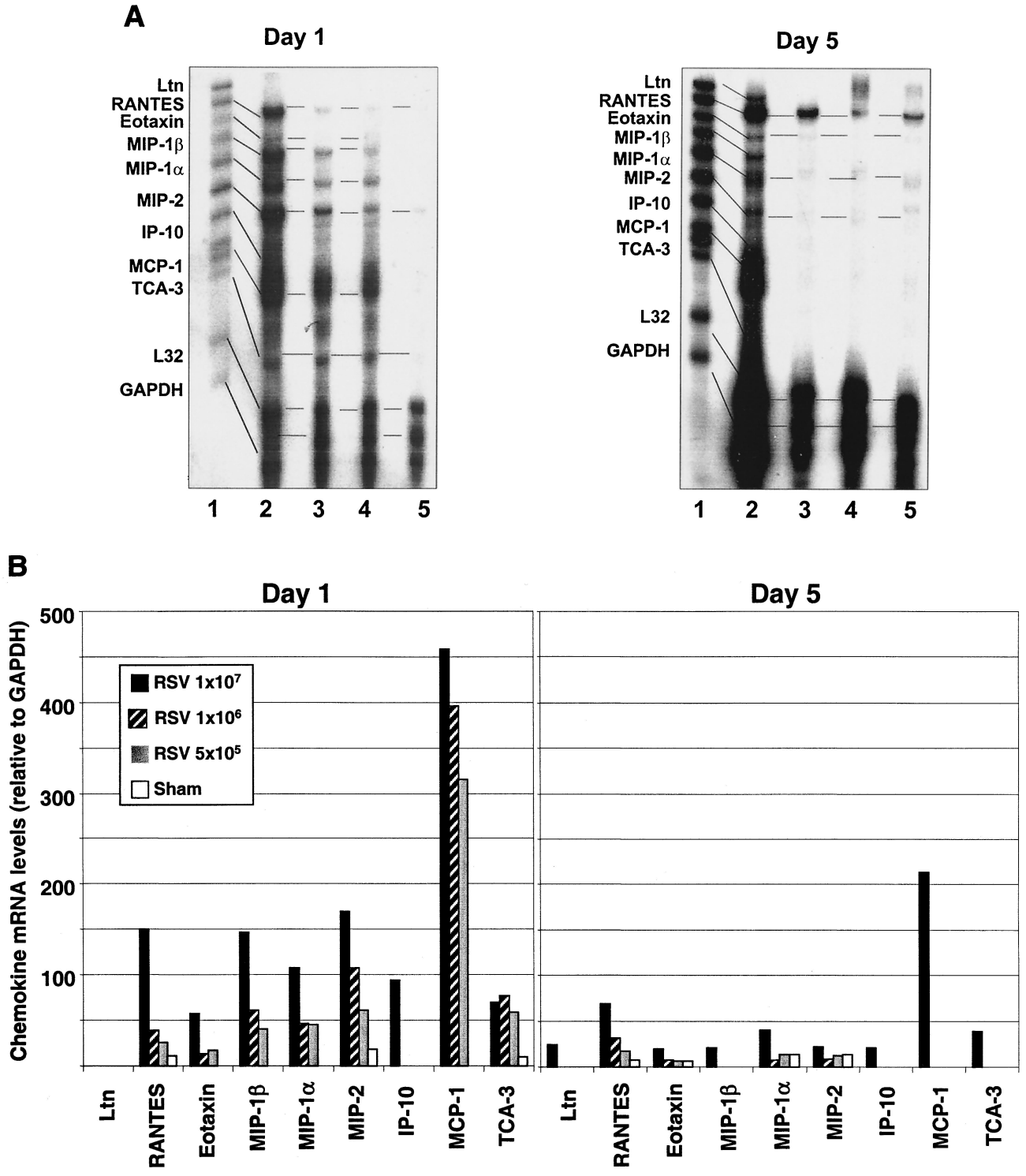

FIG. 1. Chemokine mRNA expression in lung tissue of RSV-infected BALB/c mice. Expression of nine murine chemokine mRNAs was investigated by RPA. The figure is a representative result from three independent experiments (six animals per group per experiment). (A) BALB/c mice were infected i.n. with 5×10^5 (lane 4), 10^6 (lane 3), or 10^7 (lane 2) PFU of sucrose gradient-purified RSV, or they were sham-infected with uninfected tissue culture medium (lane 5). At day 1 and 5 after infection, RNA was isolated from lung tissue and hybridized with a ^{32}P-labeled RiboQuant MultiProbe (Pharmigen) containing DNA templates for the mouse chemokines Ltn, RANTES, eotaxin, MIP-1β, MIP-1α, MIP-2, IP-10, MCP-1, TCA-3, and the house keeping genes coding for L32 (ribosomal RNA) and GAPDH. After RNAse treatment and purification, protected probes were run on a QuickPoint sequence gel, exposed to an XAR film and developed. The identity of each protected fragment was established as described in Materials and Methods. (B) The quantity of each mRNA species in the original RNA sample was determined based on the signal intensity (by optical densitometry) given by the appropriately sized, protected probe fragment band. Sample loading was normalized to the housekeeping gene GAPDH, included in each template set. The density of each chemokine mRNA on day 1 and day 5 is expressed relative to that of GAPDH.

lungs; and RPA analysis was performed using a multiprobe containing DNA templates for nine murine chemokines. In sham-infected mice, three and four mRNA-protected bands specific for RANTES, MIP-2, MIP-1α, TCA-3, and eotaxin were weakly visible at days 1 and 5, respectively (Fig. 1A, left panel). In 24-h-RSV-infected mice, we consistently observed the upregulation of mRNAs for RANTES, MIP-2, TCA-3, and eotaxin, compared to sham-inoculated animals, as well as the appearance of mRNA bands for MIP-1β, MIP-1α, IP-10, and MCP-1. The induction or upregulation of chemokine mRNAs by RSV was generally dependent on the dose of viral inoculum, with the exception of eotaxin and TCA-3. IP-10 mRNA was induced only in the lung of mice infected with the highest dose of RSV (10^7 PFU). In the latter group, a threefold average increase in lung chemokine mRNA expression compared to animals inoculated with the lowest viral dose (5×10^5 PFU) could be measured (Fig. 1B, left panel). In particular, in mice infected with 10^7 PFU, levels of RANTES and MIP-1β mRNA were approximately six- and fourfold greater, respectively, compared with those detected in mice infected with 5×10^5 PFU of RSV. Overall, the most striking finding at day 1 was the strong induction of MCP-1mRNA, whose levels of expression by far exceeded those of other inducible chemokines for all three inoculation doses.

Five days after infection, all chemokine mRNAs that were expressed on day one were still strongly detectable, although to a lesser extent, in mice infected with 10^7 PFU of RSV (Fig. 1, right panels). On the other hand, RANTES, eotaxin, MIP-1α, and MIP-2 mRNAs were drastically reduced compared to day 1, while MIP-1β, IP-10, MCP-1, and TCA-3 were no longer detectable in lung tissue of mice infected with the lower doses of RSV (5×10^5 or 10^6 PFU). Interestingly, Ltn mRNA, which was not expressed at day 1, was induced at day 5 by the highest inoculum dose of RSV. Since in the BALB/c mouse model of RSV infection maximum clinical disease (weight loss) has been reported to occur between day 5 and 10 (14), we also determined chemokine expression in lung tissue at day 8 and 11 postinfection. The profile and abundance of chemokine mRNA expression at days 8 and 11 were comparable to those described for day 5 (data not shown).

Twenty-one days postinfection, RANTES mRNA was still strongly expressed in lung tissue of mice infected with 10^7 PFU of RSV, together with much weaker bands corresponding to the eotaxin, MIP-1α, and MIP-1β mRNAs (data not shown). Expression of RANTES mRNA, but not other chemokine mRNA, was also faintly detectable in sham-inoculated mice and in mice inoculated with lower doses (5×10^5 and 10^6 PFU) of RSV.

Chemokine proteins in lungs of RSV-infected mice. To confirm that RSV-induced chemokine mRNA expression was associated with the production of chemokine proteins, we measured the concentration of RANTES, MIP-1α, and MCP-1 proteins in lung tissue and in BAL samples. We selected these chemokines based on the observations that (i) they were strongly inducible (at the mRNA level) in RSV-infected mice (Fig. 1), (ii) they are produced by human lower airway epithelial cells in vitro following RSV infection (26), and (iii) they have been shown to be present in the airway secretions of infants with RSV-induced bronchiolitis (17, 36). For these experiments, groups of BALB/c mice were infected with 5×10^5, 10^6, and 10^7 PFU of pRSV or were sham-inoculated, exactly as described for the RPA analysis. Twenty-four hours postinoculation, a time corresponding to the maximal expression of chemokine mRNAs, lungs were removed and homogenized, and after centrifugation and filtration the cleared supernatants were tested by specific ELISAs.

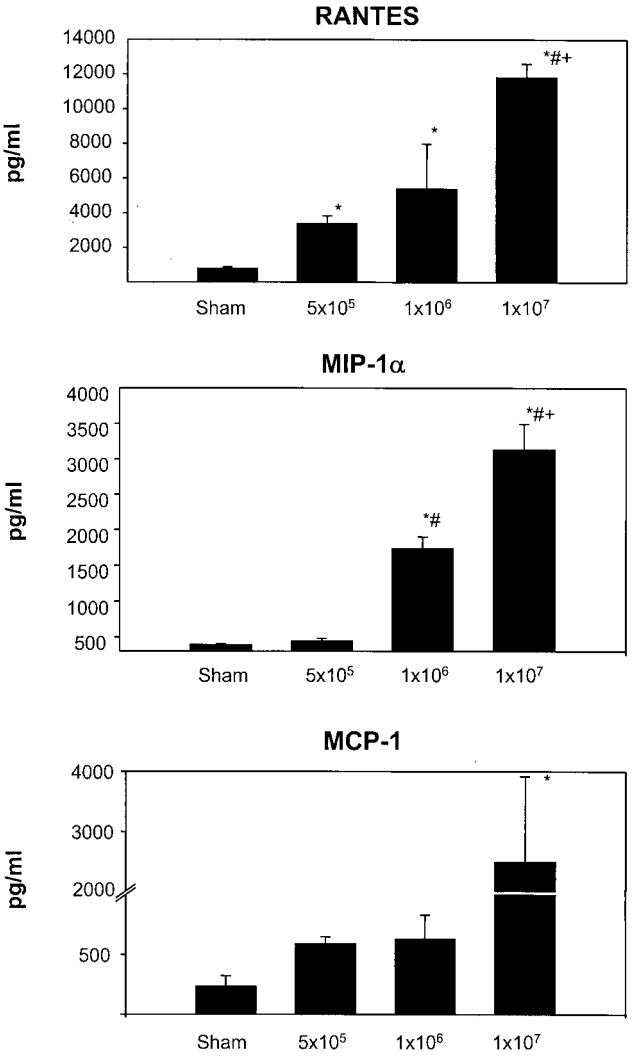

FIG. 2. Chemokine production in lung tissue of RSV-infected mice. Concentrations of RANTES, MIP-1α, and MCP-1 were determined by ELISA in lung tissue homogenate obtained from groups of sham- or RSV-infected mice (24 h). Concentrations of chemokines were adjusted for lung weight. Data are expressed as means + standard errors of the mean (error bars) of three animals per group in three independent experiments. *, $P < 0.05$ in comparison to sham-infected mice; #, $P < 0.05$ compared with mice infected with 5×10^5 PFU of pRSV; +, $P < 0.05$ in comparison to mice infected with 10^6 PFU of pRSV.

As shown in Fig. 2, RSV infection resulted in a dose-dependent production of the chemokines RANTES, MIP-1α, and MCP-1, mirroring our findings of inducible expression of chemokine mRNAs. Infection with the lowest RSV dose (5×10^5 PFU) induced a fourfold increase of RANTES protein (3,376 ± 459 pg/ml; $P = 0.005$) compared to sham-infected mice (789 ± 87 pg/ml). The increase was more pronounced in mice infected with 10^6 PFU (5,377 ± 2,582 pg/ml; $P = 0.06$)

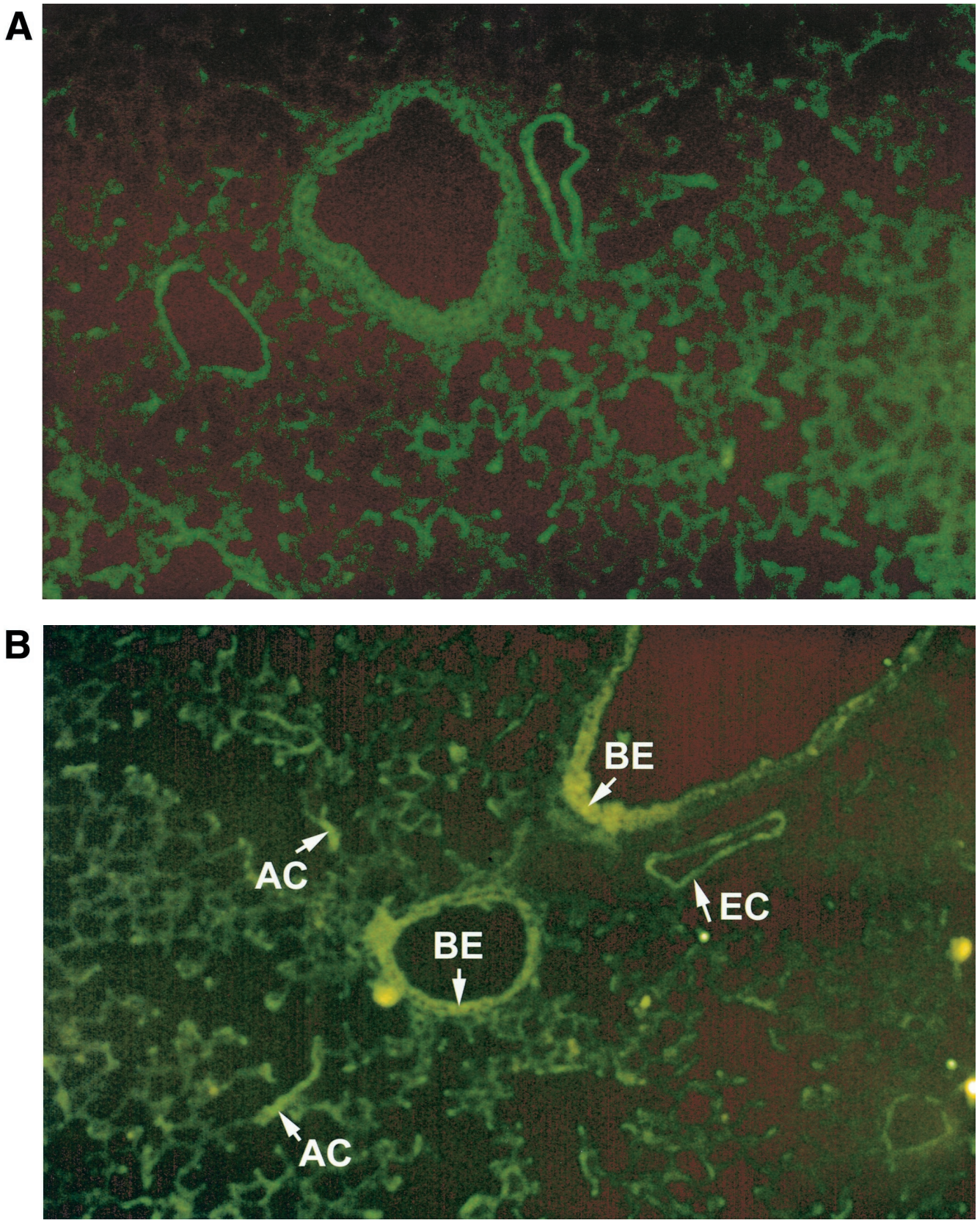

FIG. 3. Immunolocalization of MIP-1α in lung sections from RSV-infected mice. Frozen lung sections were prepared from 24-h-sham- (A) and -RSV-infected (10^7 PFU) (B and C) BALB/c mice. MIP-1α was detected by specific polyclonal goat antibody and visualized by Alexa Fluor 488-labeled donkey anti-goat IgG antibody. (A) Sham-infected mice show no evidence of specific staining (magnification, ×50). (B and C) In RSV-infected mice, bright fluorescence staining for MIP-1α appears to be localized in some alveolar epithelial cells and in epithelial cells of some bronchioles and in adjoining capillary endothelium (original magnifications, ×50 [B] and ×10 [C]). The arrows indicate positively stained epithelial cells of bronchioles (BE), endothelial cells (EC), and alveolar epithelial cells (AC).

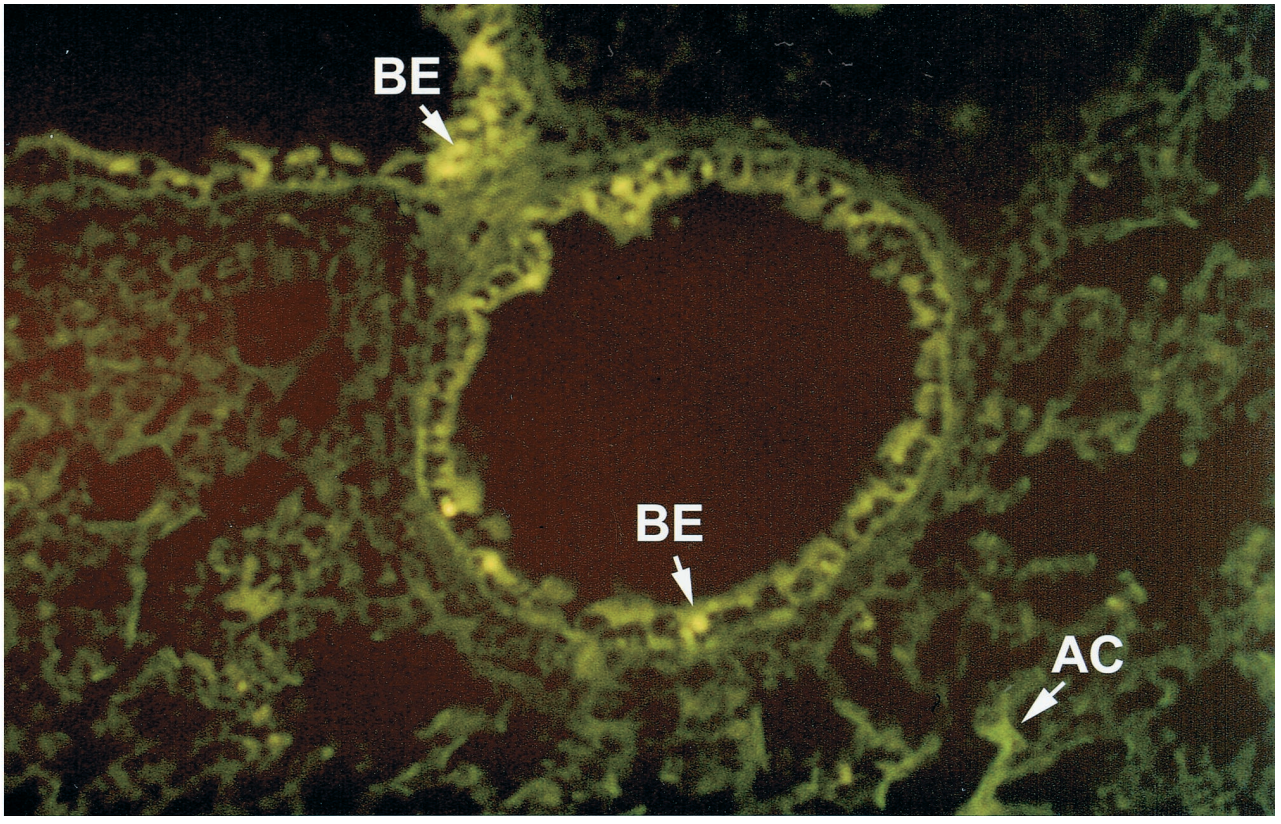

FIG. 3—*Continued.*

and 10^7 PFU (11,803 ± 792 pg/ml; $P < 0.001$) compared to sham-infected mice. MIP-1α concentrations were low in sham-infected mice (390 ± 15 pg/ml) but were significantly increased in mice infected with 10^6 PFU (1,734 ± 165 pg/ml; $P < 0.001$) or 10^7 PFU (3,130 ± 364 pg/ml; $P < 0.001$) of RSV. Inoculation with 5×10^5 PFU of RSV induced only a slight, nonsignificant increase in MIP-1α level compared to sham-inoculated animals (433 ± 39 pg/ml). MCP-1 concentrations detected in lung tissue of mice infected with 5×10^5 PFU (586 ± 61 pg/ml) or 10^6 PFU (629 ± 200 pg/ml) of RSV were always higher than those in sham-infected mice (230 ± 91 pg/ml), although these differences were not statistically significant. On the other hand, the levels of MCP-1 in mice infected with 10^7 PFU (2,127 ± 1,164 pg/ml) were significantly higher than those measured in sham-inoculated mice ($P < 0.05$).

Similarly to the findings in lung tissue extracts, RSV infection induced a dose-dependent increase in the levels of RANTES, MIP-1α, and MCP-1 in samples of BAL. The concentrations of all three chemokines were significantly higher in the BAL samples obtained from mice infected with the highest dose of RSV than in sham-infected mice ($P < 0.001$) or mice infected with 5×10^5 PFU of RSV ($P < 0.05$) (data not shown).

Immunohistochemical localization of MIP-1α. In humans, MIP-1α production appears to be selectively regionalized in the distal segments of the bronchial tree and in the lung, a site where RSV-mediated inflammation is associated with greater pathological changes, particularly in young infants (26). This is not the case for other CC chemokines such as RANTES or MCP-1, which are less selectively produced by epithelial cells of the entire respiratory tract (32). Therefore, we decided to investigate in our BALB/c mouse model if expression of MIP-1α resembled the cell distribution observed in humans. For this purpose, frozen lung tissue sections were immunostained with a specific antibody recognizing murine MIP-1α and visualized by Alexa Fluor 488-labeled donkey anti-goat IgG antibody. As shown in Fig. 3A, sham-infected mice showed no evidence of specific staining. On the other hand, in RSV-infected mice (24-h time point) fluorescence staining for MIP-1α appeared to be localized in alveolar epithelial cells, in epithelial cells of some bronchioles and in adjoining capillary endothelium (Fig. 3B and C).

Lung inflammation in RSV-infected BALB/c mice. A well-known function of chemokines is to drive leukocyte migration through tissues to target microenvironments. Therefore, the histologic appearance of the lung and the degree of inflammation, in temporal association with RSV-induced chemokine production, were investigated. Groups of 4- to 6-week-old female BALB/c mice were infected with sucrose-purified RSV preparations (5×10^5, 10^6, and 10^7 PFU) or were sham inoculated, exactly as described for the determination of chemokine expression. At day 1 and 5 postinfection, multiple H&E-stained lung sections were analyzed and inflammation was scored using a scoring scale previously described (24, 38). In sham-infected mice, few infiltrating cells were found around bronchioles or vessels (Fig. 4D and 5). Cellular infiltration around bronchioles and vessels increased with increasing doses of inoculated RSV, both at day 1 and 5 postinfection (Fig. 4A

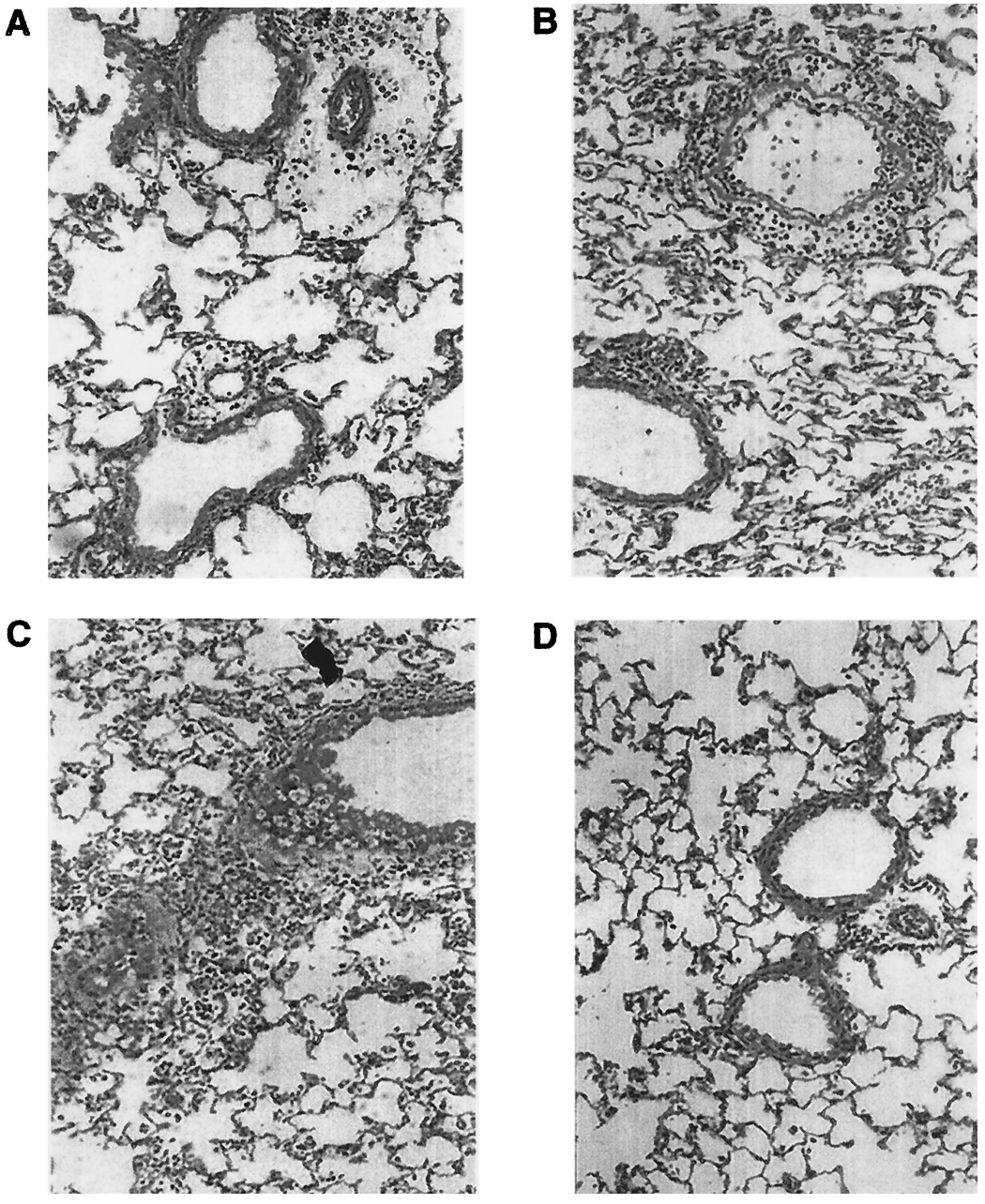

FIG. 4. Lung histopathology of BALB/c mice infected with RSV. Mice were infected i.n. with 5×10^5 PFU (A), 10^6 PFU (B), and 10^7 PFU (C) of sucrose-purified RSV or were sham infected (D). At day 1 postinfection mice were killed and lungs were removed, fixed in 10% buffered formalin, and embedded in paraffin. Multiple 4-μm-thick sections were stained with H&E. Original magnification, ×50.

to C and 5). Moreover, mice infected with the highest dose of RSV had clear evidence of diffuse increase in the number of inflammatory cells in the alveolar spaces with some areas of more severe involvement (Fig. 4C). The overall inflammation in the lung tissue was characterized by an excess of mononuclear cells (monocytes/macrophages), lymphocytes, and, to a lesser extent, neutrophils, at both day 1 and 5 postinfection (Fig. 4). Specific staining procedures did not conclusively demonstrate the presence of eosinophils in lung tissue of sham- and RSV-infected mice at any time point examined.

RSV replication and chemokine expression in lungs of BALB/c mice. To determine the relationship between viral replication in vivo and chemokine gene induction, we measured viral titers in the lungs of mice inoculated with 5×10^5, 10^6, and 10^7 PFU of sucrose-purified RSV. Figure 6 illustrates the RSV titers at day 1, 5, and 21, the time points at which chemokine expression was investigated. At day 1 (eclipse phase) RSV titers were at the lower limits of detection for all three inoculation doses. Viral replication in the lung resulted in increased titers at day 5, where nonsignificant differences were found between mice infected with 5×10^5, 10^6, or 10^7 PFU. At day 21, no virus was detectable in the lung for all inoculation doses. Statistical analysis showed that chemokine mRNA abundance and protein levels did not correlate with

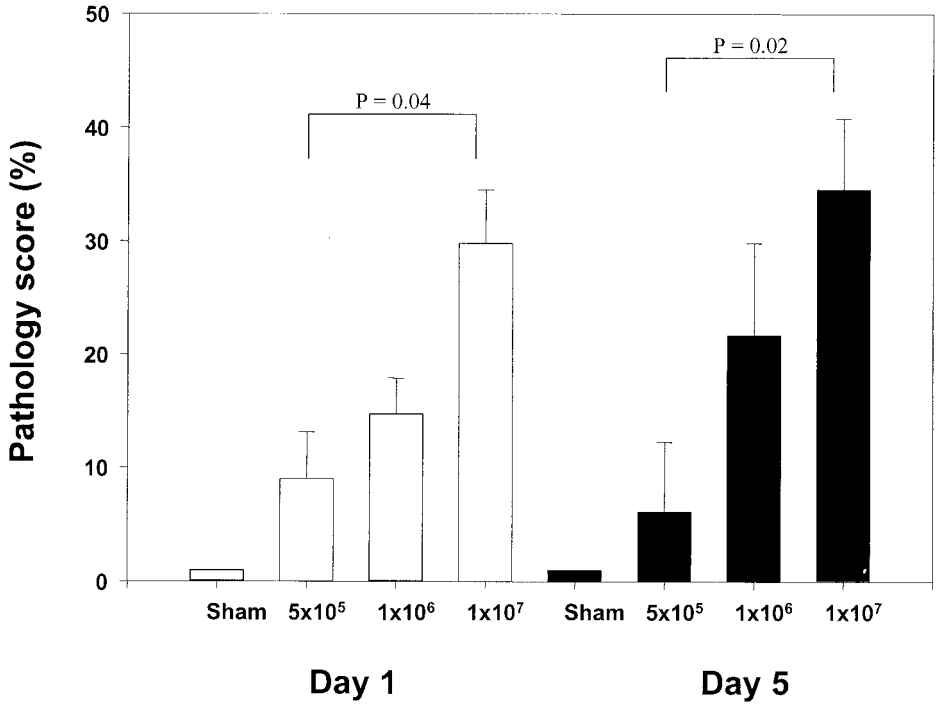

FIG. 5. Pathology scores in RSV-infected BALB/c mice. Mice were infected i.n. with 5×10^5, 10^6, and 10^7 PFU of sucrose-purified RSV or were sham infected. At day 1 (white bars) and 5 (black bars) postinfection multiple lung sections were stained with H&E. Inflammation was scored blindly by two independent investigators. The number of abnormal perivascular and peribronchial spaces divided by the total spaces counted is the percentage reported as the pathology score (see Materials and Methods). The figure presents the data of two independent experiments with total of five mice per group (mean + standard error of the mean [error bars]).

viral titers, both at day 1 and 5. Therefore, since the dose of RSV inoculum appeared to be a critical factor associated with the early production of chemokines (day 1) as well as their long-lasting inducible expression (days 5 to 11), we investigated the role of RSV replication in this process. In this experiment, BALB/c mice were inoculated either with intact sucrose-purified RSV or with a UV-inactivated preparation of RSV (both at a dose of 10^7 PFU) and the expression of chemokine mRNA was determined by RPA. Lack of replication of the UV-treated RSV preparation was confirmed before inoculation and in lung tissue by a plaque assay. At 24 h, mice inoculated with UV-treated RSV expressed mRNA for the chemokines RANTES, MIP-1α, MIP-1β, MIP-2, and MCP-1, although in much lower abundance compared to mice infected with intact replicating virus (Fig. 7). On the other hand, eotaxin, IP-10, and TCA-3 were not detectable in mice inoculated with UV-RSV (Fig. 7).

Chemokine expression, viral titer, and lung inflammation in MIP-1α-deficient mice. Studies of infants with naturally acquired RSV infection, suggest that MIP-1α may play an important role in the pathogenesis of severe lower airway disease (17). Therefore, we determined lung chemokine expression and the degree of inflammation in mice in which the gene encoding for MIP-1α was disrupted (6). MIP-1α-deficient mice (−/− mice) and control littermates (+/+ mice) were inoculated i.n. with RSV (10^7 PFU) or PBS (sham). Five days after infection mice were sacrificed and the expression of lung chemokine mRNAs, degree of inflammation and viral titer were determined exactly as described for BALB/c mice. In sham-inoculated +/+ and −/− mice, only a single band specific for RANTES mRNA was detected by RPA. In RSV-infected +/+ mice the profile of chemokine expression was comparable to that observed in BALB/c mice (i.e., Ltn, RANTES, eotaxin, MIP-1β, MIP-1α, MIP-2, IP-10, MCP-1, and TCA-3). In RSV-infected MIP-1α −/− mice Ltn mRNA was not expressed and there was a trend for a reduced expression of RANTES, MIP-2, and MCP-1 compared to that in +/+ control animals. As expected, MIP-1α mRNA was not expressed in sham- or RSV-infected −/− mice (Fig. 8).

Similarly to BALB/c mice, the lungs of RSV-infected MIP-1α +/+ mice had evident signs of inflammation, with abundant infiltration of mononuclear cells around 80% of the bronchioles and vessels scored and in alveolar spaces (Fig. 9A). On the other hand, in RSV-infected −/− mice none of the scored bronchioles and vessels had scores of >3 (Fig. 9B). However, viral replication was not significantly different at the time point analyzed (day 5 postinfection, four mice from each group) in the lungs of RSV-infected −/− mice (2.62 ± 0.1 $\log_{10}$ PFU/g of tissue) compared to +/+ mice (2.1 ± 0.3 $\log_{10}$ PFU/g of tissue)($P = 0.1$).

DISCUSSION

Numerous studies in vitro have demonstrated that RSV is a potent inducer of chemokine production in infected human respiratory epithelial cells. Indirect evidence suggests that these inflammatory molecules may play a critical role in the pathogenesis of RSV disease in infants. Greater concentrations of MIP-1α and RANTES have been demonstrated in nasopharyngeal secretions and tracheal aspirates of infants with RSV bronchiolitis in comparison to respiratory-disease-

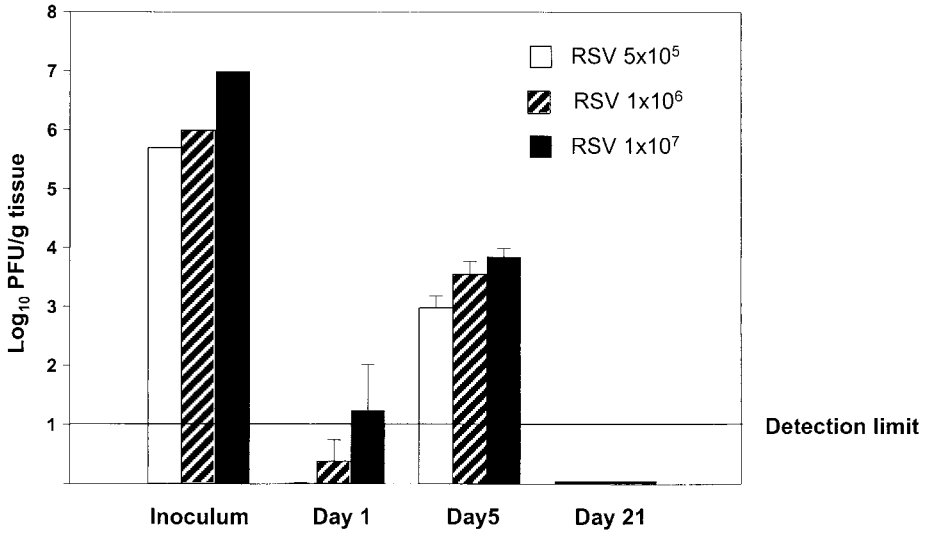

FIG. 6. Viral replication in lung of BALB/c mice infected with sucrose-purified RSV. BALB/c mice (five animals per group) were infected i.n. with 5×10^5, 10^6, or 10^7 PFU of RSV (indicated as inoculum). One, five, and twenty-one days after infection, lung tissue was removed and homogenized and the concentration of infectious virus was determined by plaque assay. The mean $\log_{10}$ titer (PFU) per gram of tissue + standard error of the mean (error bar) is shown. The lower detection limit is indicated.

free children (36). Greater quantities of MIP-1α and RANTES were also found in infants intubated because of RSV infection than in control infants that were intubated for nonrespiratory illnesses (17). We have recently extended these findings, by showing that in comparison to subjects with upper respiratory infections, subjects with bronchiolitis have higher concentrations of MIP-1α and eotaxin in nasopharyngeal secretions, both of which are associated with the development of more severe forms of illness due to RSV (unpublished data). In the present study, we provide novel experimental evidence that

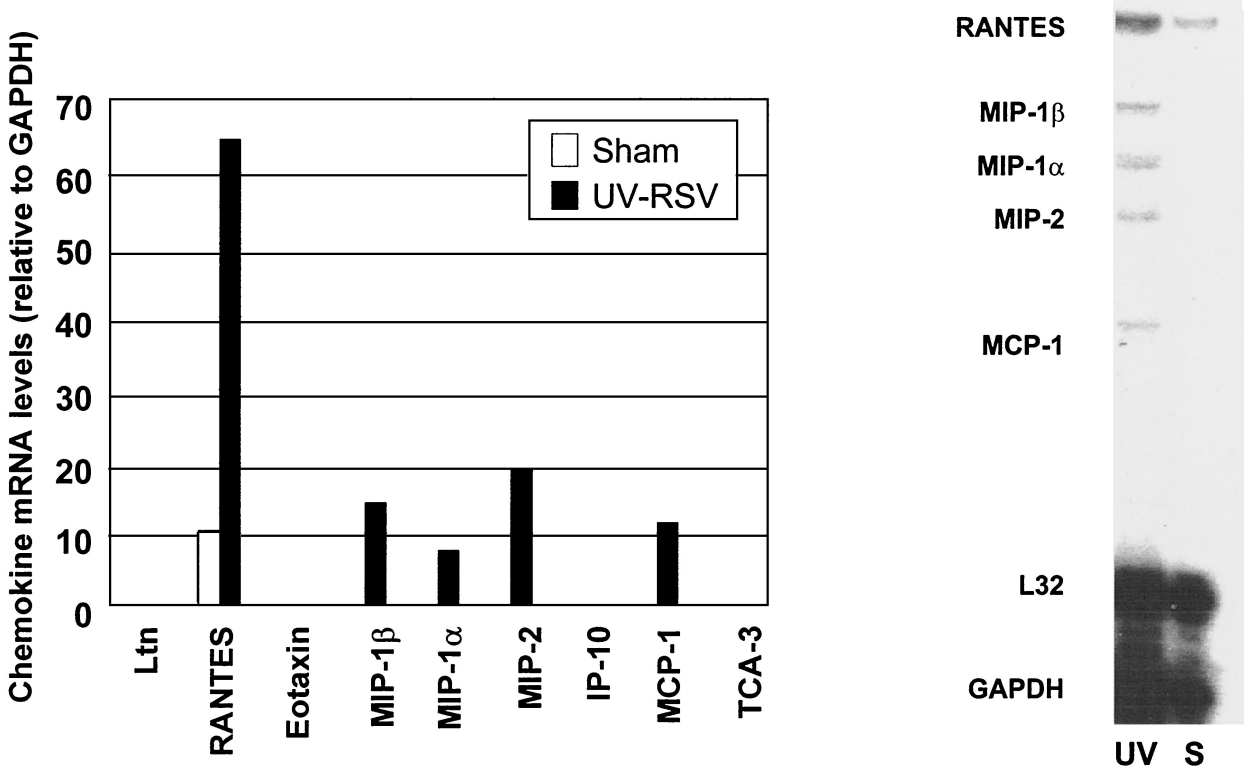

FIG. 7. Chemokine mRNA expression in lung of mice inoculated with UV-inactivated RSV. BALB/c mice were inoculated i.n. with UV-inactivated purified RSV (10^7 PFU) (lane UV), or they were sham-infected (lane S). At day 1 after infection, chemokine mRNA expression was determined by RPA as described in the legend to Fig. 1. The figure is a representative result from three animals per group.

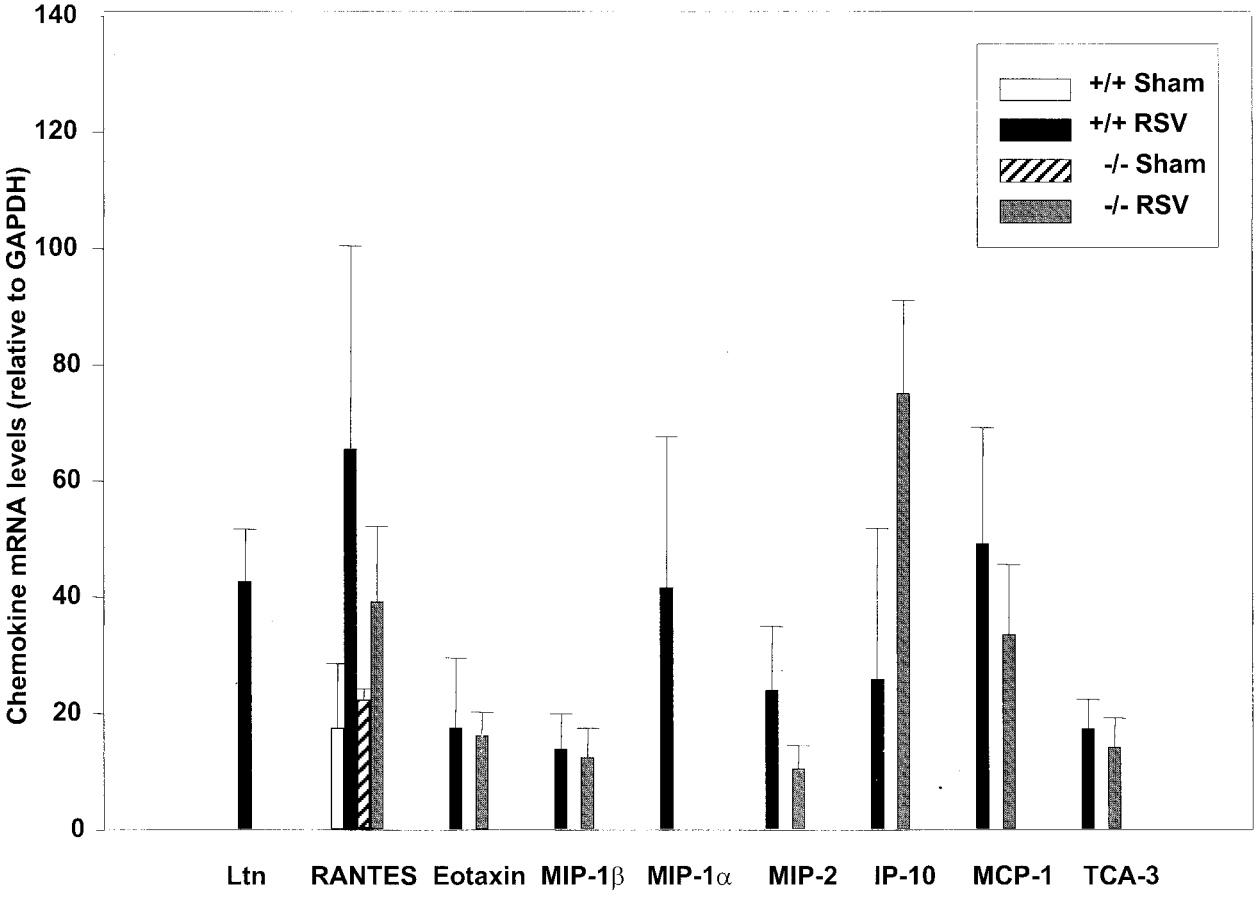

FIG. 8. Chemokine mRNA expression in lung tissue of RSV-infected MIP-1$\alpha^{-/-}$ mice. Expression of chemokine mRNA was determined exactly as described in the legend to Fig. 1. MIP-1$\alpha^{-/-}$ mice (−/−) and control littermates (+/+) were infected i.n. with 10^7 PFU of purified RSV, or they were sham inoculated. At day 5 after infection, extracted lung RNA was analyzed by RPA. The density of each chemokine mRNA in RSV-infected MIP-1$\alpha^{-/-}$ and MIP-1$\alpha^{+/+}$ mice is expressed relative to that of GAPDH. The data are expressed as means + standard errors of the means (error bars) of four animals per group.

chemokines are critically involved in RSV-mediated lung inflammation, an essential pathogenic component of RSV infection. Supporting our conclusion are the following findings. (i) Experimental RSV infection of BALB/c mice results in the inducible expression of lung ELR-containing (MIP-2) and non-ELR-containing (IP-10) CXC chemokines, CC chemokines (RANTES, MIP-1α, MIP-1β, MCP-1, TCA-3), and the C chemokine Ltn. (ii) Virus dose-dependent induction of chemokines is associated with the dose-dependent appearance of lung cellular inflammation. (iii) Genetically altered mice lacking the MIP-1α gene (−/−) have substantial reduction of airway inflammation following RSV infection compared to their control littermates (+/+).

The profile of the inducible lung chemokines shown in this study closely reflects the type of cellular infiltration, dictated by the cell distribution of chemokine receptors, which is characteristic of the RSV-infected mouse model (14, 41). In this regard, the CCR1- and CCR5-binding chemokines RANTES, MIP-1α, and MIP-1β are potent chemoattractants for monocytes and activated T cells (both $CD4^+$ and $CD8^+$) (34, 40). MCP-1, which binds to the CCR2 receptor, is a potent chemoattractant and activator of monocytes (31) and is involved in macrophage activation leading to the release of inflammatory mediators and tissue damage (15). Neutrophils, which represent a sizeable component of the inflammatory infiltrate in RSV infection, are strongly susceptible to the chemotactic effect of MIP-2, a mouse homologue of IL-8 (9), and, surprisingly for a member of the CC chemokine family, to TCA-3 (23). NK cells, whose activity peaks during the first days of primary RSV infection, express a number of chemokine receptors that allow them to respond to several chemokines, including IP-10, lymphotactin, RANTES, MIP-1α, and MCP-1 (reviewed in reference 33).

Despite the fact that the CC chemokines eotaxin, RANTES, and MIP-1α are known to be potent chemoattractants for eosinophils, we were unable to demonstrate eosinophils in the lung of RSV-infected BALB/c mice. These data are consistent with several other studies with nonsensitized, nonvaccinated mice infected with RSV (i.e., primary infection) (27) and suggest that eosinophil-attracting chemokines may be necessary but not sufficient to fully activate the multistep process required for migration of eosinophils into lung tissue. In this regard, the eosinophil growth factors IL-5 and GM-CSF play an essential role in mediating eosinophil infiltration in mouse asthma models (11, 39), while selective deletion of the eosinophil-specific eotaxin gene has shown partial or no effect on

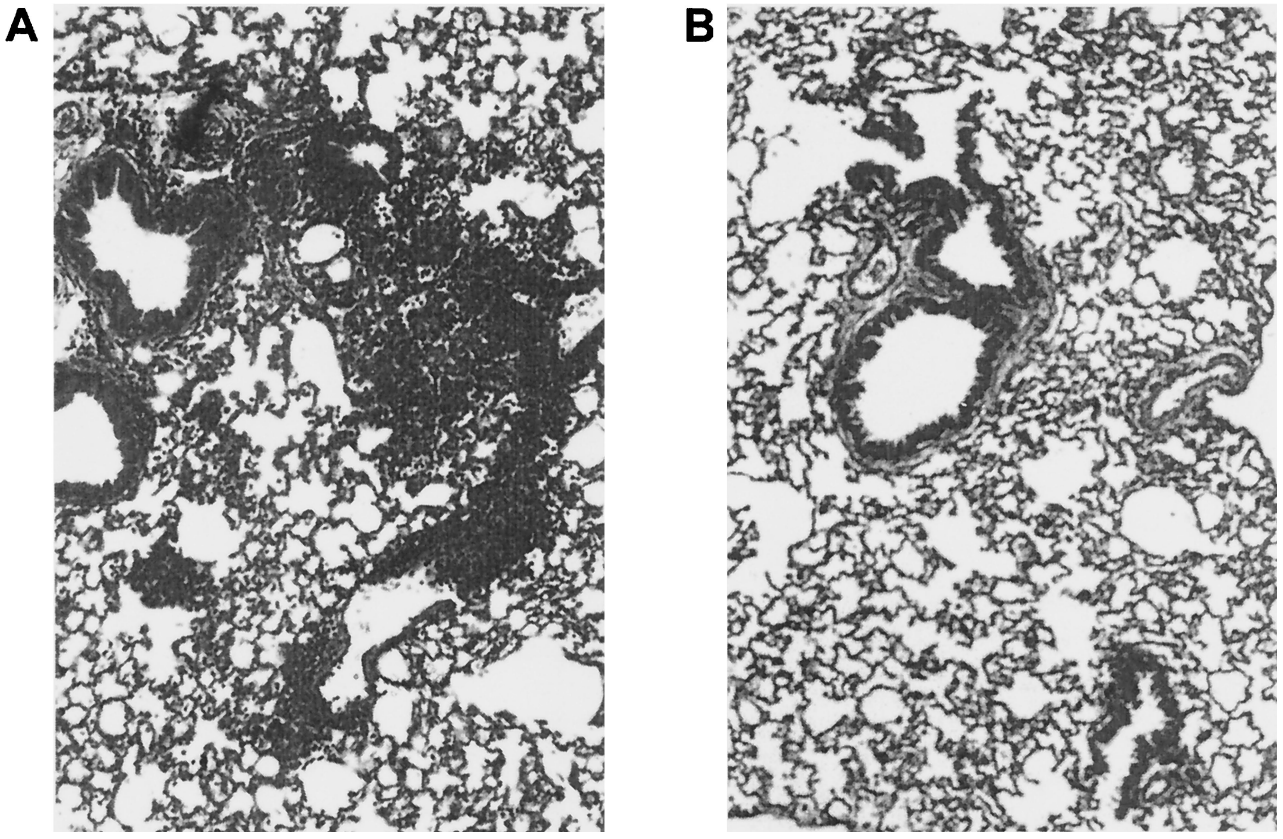

FIG. 9. Lung histopathology of RSV-infected MIP-1$\alpha^{-/-}$ mice. MIP-1$\alpha^{-/-}$ mice and control littermates were infected i.n. with 10^7 PFU of sucrose gradient-purified RSV or were sham inoculated. At day 5 postinfection lung sections were stained with H&E and inflammation was scored as described in Materials and Methods. A representative section is shown from a +/+ control mouse (A) and from a −/− mouse (B). Original magnification, ×50.

eosinophil recruitment (47). Although one group has described IL-5-dependent eosinophil lung infiltration in a mouse model of RSV infection (35), there is no strong experimental evidence that either IL-5 or GM-CSF is induced in the airways of mice following primary RSV infection. On the other hand, the production of GM-CSF by RSV-infected human epithelial cells (25) may explain why infants with naturally acquired RSV bronchiolitis show evidence of activated eosinophils in their airway mucosa (12) as well as a positive correlation between the concentrations of eosinophil-specific proteins and those of MIP-1α in respiratory secretions (17). An interesting finding in this study was the demonstration of a difference in profile of chemokines induced in the lung by replicating versus inactivated purified preparations of RSV. Eotaxin, IP-10, and TCA-3 required viral replication in the lung for their expression, while RANTES, MIP-1β, MIP-1α, MIP-2, and MCP-1 were inducible by inoculation of the mice with inactivated RSV, although in much lower abundance compared to mice infected with intact virus. Since the preparations of RSV used in our protocol were sucrose purified and therefore devoid of a number of contaminating mediators normally present in infected tissue culture preparations (i.e., crude, nonpurified virus) (18), these results suggest that certain cellular components of the lung are able to respond, either directly to RSV particle binding or indirectly via intermediate mediators released by other cells. While expression of chemokine and cytokine genes in epithelial cells has been extensively shown to require viral replication (reviewed in reference 13), in other cell types, including macrophages (2), neutrophils (21), and eosinophils (R. Garofalo, personal observation), binding of nonreplicating RSV particles or virus-specific surface proteins appears to be able to induce production of certain chemokines and cytokines. These in vitro studies are, however, restricted to single cell types and do not provide insights into the mechanisms that regulate in vivo airborne-pathogen-mediated propagation of inflammatory signals from the airspace to the vascular space. In elegant studies, Kuebler et al. have recently shown that an alveolar stimulus, restricted to the epithelial cells, induced a rapid Ca^{2+} signaling in endothelial cells of perialveolar capillaries, leading to the expression of leukocyte-endothelium adhesion molecules (22). It is tempting to speculate that RSV, irrespective of its ability to fully replicate in lung epithelial cells, may be able to rapidly trigger intercompartmental signaling that leads to the expression of certain chemokine genes in other tissue resident cells, such as endothelial cells. Supporting this hypothesis is our observation that the expression of MIP-1α was identified by immunohistochemistry in airway epithelial cells and in the adjacent capillary endothelial cells, a cell type not known to be directly susceptible to RSV infection (Fig. 3). The implication in vivo of these observations is not fully understood at the present moment.

Although several chemokines were induced in the lung of

RSV-infected mice, our results indicate that the CC chemokine MIP-1α may play a central role in mediating RSV-induced inflammatory process of the airways. Following RSV infection, mice genetically deficient for the MIP-1α gene had significant reduction of total lung cellular inflammation compared to control littermates, without obvious differences in viral replication. Similar results in virus-induced models of lung, myocardium, and cornea inflammation have been previously reported in MIP-1α$^{-/-}$ mice infected with influenza, pneumonia virus of mice, coxsackievirus, and herpes simplex virus, respectively (6, 7, 42). In those studies viral clearance was either delayed (6, 7) or unaffected (42) compared to that in +/+ animals. Our observation that RSV-infected MIP-1α$^{-/-}$ mice showed a trend for reduced levels of RANTES, MIP-2, and MCP-1 mRNA, compared to +/+ mice is also in agreement with a previous report (42): the functional significance of this observation, in the contest of MIP-1α-mediated lung inflammation, is currently unknown.

In conclusion, our studies demonstrate that chemokines, and MIP-1α in particular, are critically involved in the pathogenesis of lung inflammation in mice experimentally infected with RSV. The results presented herein extend previous observations in vitro and support other indirect evidence of the involvement of lung chemokines in the clinical manifestations of naturally acquired RSV infection (bronchiolitis). Additional studies are under way to determine the role of lung chemokines in mediating other pathophysiologic features of RSV infection, such as airway hyperresponsiveness.

ACKNOWLEDGMENTS

This work was supported by grant AI 15939 from the National Institutes of Health, by grant 644-0-0 of the Fortune Program of the University of Tuebingen, Tuebingen, Germany, and by a grant of the John Sealy Memorial Endowment Fund for Biomedical Research at UTMB.

We thank Todd Elliott for excellent technical assistance. We are grateful to Allan Brasier, Sanjiv Sur, and James Wild for helpful discussions and to Klaus Unertl for his invaluable support.

REFERENCES

1. **Aherne, W. T., T. Bird, S. D. B. Court, P. S. Gardner, and J. McQuillin.** 1970. Pathological changes in virus infections of the lower respiratory tract in children. J. Clin. Pathol. **23:**7–18.
2. **Becker, S., J. Quay, and J. Soukup.** 1991. Cytokine (tumor necrosis factor, IL-6, and IL-8) production by respiratory syncytial virus-infected human alveolar macrophages. J. Immunol. **147:**4307–4312.
3. **Becker, S., W. Reed, F. W. Henderson, and T. L. Noah.** 1997. RSV infection of human airway epithelial cells causes production of the beta-chemokine RANTES. Am. J. Physiol. **272:**L512–L520.
4. **Buckinham, S. C., A. J. Bush, and J. P. Devincenzo.** 2000. Nasal quantity of respiratory syncytial virus correlates with disease severity in hospitalized infants. Pediatr. Infect. Dis. **19:**113–117.
5. **Chanock, R. M., K. McIntosh, B. R. Murphy, and R. H. Parrott.** 1991. Respiratory syncytial virus, p. 525–544. *In* A. S. Evans (ed.), Viral infections of humans. Plenum Publishing Corporation, New Haven, Conn.
6. **Cook, D. N., M. A. Beck, T. M. Coffman, S. L. Kirby, J. F. Sheridan, I. B. Pragnell, and O. Smithies.** 1995. Requirement of MIP-α for an inflammatory response to viral infection. Science **269:**1583–1585.
7. **Domachowske, J. B., C. A. Bonville, J.-L. Gao, P. M. Murphy, A. J. Easton, and H. F. Rosenberg.** 2000. The chemokine macrophage-inflammatory protein-1*alpha* and its receptor CCR1 control pulmonary inflammation and antiviral host defense in paramyxovirus infection. J. Immunol. **165:**2677–2682.
8. **Downham, M. A. P. S., P. S. Gardner, and J. McQuillin.** 1975. Role of respiratory viruses in childhood mortality. Br. Med. J. **1:**235–239.
9. **Driscoll, K. E.** 1994. Macrophage inflammatory proteins: biology and role in pulmonary inflammation. Exp. Lung Res. **20:**473–490.
10. **Ferris, J. A., W. A. Aherne, and W. S. Locke.** 1973. Sudden and unexpected deaths to infants: histology and virology. Br. Med. J. **2:**439–449.
11. **Foster, P. S., S. P. Hogan, A. J. Ramsay, K. I. Matthei, and I. G. Young.** 1996. Interleukin 5 deficiency abolishes eosinophilia, airways hyperreactivity, and lung damage in a mouse asthma model. J. Exp. Med. **183:**195–201.
12. **Garofalo, R. P., J. L. L. Kimpen, R. C. Welliver, and P. L. Ogra.** 1992. Eosinophil degranulation in the respiratory tract during naturally acquired respiratory syncytial virus infection. J. Pediatr. **120:**28–32.
13. **Garofalo, R. P., R. C. Welliver, and P. L. Ogra.** 1999. Clinical aspects of bronchial reactivity and cell-virus interaction, p. 1223–1237. *In* P. L. Ogra, M. E. Lamm, J. Bienenstock, J. Mestecky, W. Strober, and J. R. McGhee (ed.), Mucosal Immunology. Academic Press, San Diego, Calif.
14. **Graham, B. S., M. D. Perkins, P. F. Wright, and D. T. Karzon.** 1988. Primary respiratory syncytial virus infection in mice. J. Med. Virol. **26:**153–162.
15. **Gunn, M. D., N. A. Nelken, X. Liao, and L. T. Williams.** 1997. Monocyte chemoattractant protein-1 is sufficient for the chemotaxis of monocytes and lymphocytes in transgenic mice but requires an additional stimulus for inflammatory activation. J. Immunol. **158:**376–383.
16. **Hall, C. B.** 1976. Respiratory syncytial virus infection in infants: quantitation and duration of shedding. J. Pediatr. **89:**11–15.
17. **Harrison, A. M., C. A. Bonville, H. F. Rosenberg, and J. B. Domachowske.** 1999. Respiratory syncytical virus-induced chemokine expression in the lower airways: eosinophil recruitment and degranulation. Am. J. Respir. Crit. Care Med. **159:**1918–1924.
18. **Jamaluddin, M., R. P. Garofalo, P. L. Ogra, and A. R. Brasier.** 1996. Inducible translational regulation of the NF-IL6 transcription factor by respiratory syncytial virus infection in pulmonary epithelial cells. J. Virol. **70:**1554–1563.
19. **Kelner, G. S., J. Kennedy, K. B. Bacon, S. Kleyensteuber, D. A. Largaespada, N. A. Jenkins, N. G. Copeland, J. F. Bazan, K. W. Moore, T. J. Schall, et al.** 1994. Lymphotactin: a cytokine that represents a new class of chemokine. Science **266:**1395–1399.
20. **Kisch, A. L., and K. M. Johnson.** 1963. A plaque assay for respiratory syncytial virus. Proc. Soc. Exp. Biol. Med. **112:**583.
21. **Konig, B., T. Krusat, H. J. Streckert, and W. Konig.** 1996. IL-8 release from human neutrophils by the respiratory syncytial virus is independent of viral replication. J. Leukoc. Biol. **60:**253–260.
22. **Kuebler, W. M., K. Parthasarathi, P. M. Wang, and J. Bhattacharya.** 2000. A novel signaling mechanism between gas and blood compartments of the lung. J. Clin. Investig. **105:**905–913.
23. **Luo, Y., J. Laning, S. Devi, J. Mak, T. J. Schall, and M. E. Dorf.** 1994. Biologic activities of the murine beta-chemokine TCA3. J. Immunol. **153:**4616–4624.
24. **Murphy, B. R., A. Sotnikov, P. R. Paradiso, et al.** 1989. Immunization of cotton rats with the fusion (F) and large (G) glycoproteins of respiratory syncytial virus (RSV) protects against RSV challenge without potentiating RSV disease. Vaccine **7:**533–540.
25. **Noah, T. L., and S. Becker.** 1993. Respiratory syncytial virus-induced cytokine production by a human bronchial epithelial cell line. Am. J. Physiol. **265:**L472–L478.
26. **Olszewska-Pazdrak, B., A. Casola, T. Saito, R. Alam, S. E. Crowe, F. Mei, P. L. Ogra, and R. P. Garofalo.** 1998. Cell-specific expression of RANTES, MCP-1, and MIP-1α by lower airway epithelial cells and eosinophils infected with respiratory syncytial virus. J. Virol. **72:**4756–4764.
27. **Openshaw, P. J. M.** 1995. Immunopathological mechanisms in respiratory syncytial virus disease. Springer Semin. Immunopathol. **17:**187–201.
28. **Oppenheim, J. J., C. O. C. Zachariae, N. Mukaida, and K. Matsushima.** 1991. Properties of the novel proinflammatory supergene 'intercrine' cytokine family. Annu. Rev. Immunol. **9:**617–648.
29. **Peebles, R. S., Jr., J. R. Sheller, J. F. Johnson, D. B. Mitchell, and B. S. Graham.** 1999. Respiratory syncytial virus infection prolongs methacholine-induced airway hyperresponsiveness in ovalbumin-sensitized mice. J. Med. Virol. **57:**186–192.
30. **Qin, S., J. B. Rottman, P. Myers, N. Kassam, M. Weinblatt, M. Loetscher, A. E. Koch, B. Moser, and C. R. Mackay.** 1998. The chemokine receptors CXCR3 and CCR5 mark subsets of T cells associated with certain inflammatory reactions. J. Clin. Investig. **101:**746–754.
31. **Rollins, B. J., T. Yoshimura, E. J. Leonard, and J. Pober.** 1990. Cytokine-activated human endothelial cells synthesize and secrete monocyte chemoattractant protein, MCP-1. Am. J. Pathol. **136:**1229–1233.
32. **Saito, T., R. W. Deskin, A. Casola, H. Haeberle, B. Olszewska, P. B. Ernst, R. Alam, P. L. Ogra, and R. Garofalo.** 1997. Respiratory syncytial virus induces selective production of the chemokine RANTES by upper airway epithelial cells. J. Infect. Dis. **175:**497–504.
33. **Sallusto, F., A. Lanzavecchia, and C. R. Mackay.** 1998. Chemokines and chemokine receptors in T-cell priming and Th1/Th2-mediated responses. Immunol. Today **19:**568–574.
34. **Schall, T. J., K. Bacon, R. D. Camp, J. W. Kaspari, and D. V. Goeddel.** 1993. Human macrophage inflammatory protein alpha (MIP-1 alpha) and MIP-1beta chemokines attract distinct populations of lymphocytes. J. Exp. Med. **177:**1821–1826.
35. **Schwarze, J., G. Cieslewicz, E. Hamelmann, A. Joetham, L. D. Shultz, M. C. Lamers, and E. W. Gelfand.** 1999. IL-5 and eosinophils are essential for the development of airway hyperresponsiveness following acute respiratory syncytial virus infection. J. Immunol. **162:**2997–3004.

36. **Sheeran, P., H. Jafri, C. Carubelli, J. Saavedra, C. Johnson, K. Krisher, P. J. Sanchez, and M. O. Ramilio.** 1999. Elevated cytokine concentrations in the nasopharyngeal and tracheal secretions of children with respiratory syncytial virus disease. Pediatr. Infect. Dis. J. **18:**115–122.
37. **Sigurs, N., R. Bjarnason, and F. Sigurbergsson.** 1994. Eosinophil cationic protein in nasal secretion and in serum and myeloperoxidase in serum in respiratory syncytial virus bronchiolitis: relation to asthma and atopy. Acta Paediatr. **83:**1151–1155.
38. **Stack, A. M., R. Malley, R. A. Saladino, J. B. Montana, K. L. MacDonald, and D. C. Molrine.** 2000. Primary respiratory syncytial virus infection: pathology, immune response, and evaluation of vaccine challenge strains in a new mouse model. Vaccine **18:**1412–1418.
39. **Stampfli, M. R., R. E. Wiley, G. S. Neigh, B. U. Gajewska, X.-F. Lei, D. P. Snider, Z. Xing, and M. Jordana.** 1998. GM-CSF transgene expression in the airway allows aerosolized ovalbumin to induce allergic sensitization in mice. J. Clin. Investig. **102:**1704–1714.
40. **Taub, D. D., K. Conlon, A. R. Lloyd, J. J. Oppenheim, and D. J. Kelvin.** 1993. Preferential migration of activated CD4+ and CD8+ T cells in response to MIP-1*alpha* and MIP-1*beta*. Science **260:**355–358.
41. **Taylor, G., E. J. Stott, M. Hughes, and A. P. Collins.** 1984. Respiratory syncytial virus infection in mice. Infect. Immun. **43:**649–655.
42. **Tumpey, T. M., H. Cheng, D. N. Cook, O. Smithies, J. E. Oakes, and R. N. Lausch.** 1998. Absence of macrophage inflammatory protein-1α prevents the development of blinding herpes stromal keratitis. J. Virol. **72:**3705–3710.
43. **Ueba, O.** 1978. Respiratory syncytial virus: I. Concentration and purification of the infectious virus. Acta Med. Okayama **32:**265–272.
44. **van Schaik, S. M., G. Enhorning, I. Vargas, and R. C. Welliver.** 1998. Respiratory syncytial virus affects pulmonary function in BALB/c mice. J. Infect. Dis. **177:**269–276.
45. **Volovitz, B., R. C. Welliver, G. DeCastro, D. A. Krystofik, and P. L. Ogra.** 1988. The release of leukotrienes in the respiratory tract during infection with respiratory syncytial virus: role in obstructive airway disease. Pediatr. Res. **24:**504–507.
46. **Welliver, R. C., D. T. Wong, M. Sun, E. Middleton, Jr., R. S. Vaughan, and P. L. Ogra.** 1981. The development of respiratory syncytial virus-specific IGE and the release of histamine in nasopharyngeal secretions after infection. N. Engl. J. Med. **305:**841–846.
47. **Yang, Y., J. Loy, R.-P. Ryseck, D. Carrasco, and R. Bravo.** 1998. Antigen-induced eosinophilic lung inflammation develops in mice deficient in chemokine eotaxin. Blood **92:**3912–3923.